IOSR Journal of Electrical and Electronics Engineering (IOSR-JEEE)
e- ISSN: 2278-1676, p- ISSN: 2320-3331, Volume 10, Issue 3 Ver. III (May – Jun. 2015), PP 36-44
www.iosrjournals.org

Electromagnetic Plane Waves Scattering from an Anisotropic Chiral coated Conducting Cylinder using Mie's Approach

Sajid Mumtaz[1], Abdul Ghaffar[2], Baqir Ali[3], Mubeen Aslam[4]
[1, 3] *(Department of Electronic Engineering, International Islamic University Islamabad, Pakistan)*
[2] *(Department of Electrical Engineering, King Saud University, Saudi Arabia)*
[2] *(Department of Physics, University of Agriculture, Faisalabad, Pakistan)*
[4] *(Department of Computer Science, National Textile University, Faisalabad, Pakistan)*

***Abstract**: The scattering properties of a conducting cylinder coated with an anisotropic chiral material have been investigated by using Mie's approach. By using the boundary conditions across the free space, anisotropic chiral layer and the perfect electric conductor interfaces, a set of six equations having six unknowns scattered coefficients are obtained which are solved numerically by Cramer's rule. The influence of chirality, permittivity, and permeability on differential scattering cross section and the variations with respect to different parameters are studied. The numerical results of the electromagnetic scattering response are presented. Uniaxial chiral layer is a special case for chiral material. The knowledge gained by this study is useful in many applications such as biological studies, medicine, telecommunication, meteorological studies etc. The results are compared with available literatures which are in good agreement under special conditions.*

***Keywords:** Scattering, Perfect Electric Conductor, Chiral Material, Co-polarized, Cross-polarized, Scattering Cross-section.*

I. Introduction

For the last many years, the materials made up of chiral objects have proved their worth in the electromagnetic field theory. A chiral object is a three-dimensional body that cannot be brought into congruence with its mirror image by translation or rotation [1].In the current treatise, the effects of permittivity and permeability on anisotropic chiral layer in co- and cross polarized modes have been examined using Mie's analysis. It is demonstrated that a uniaxial chiral material can be used as a polarization transformer [2, 3, 4]. Hulst [5] used Mie's approach [6] for the analysis of both dielectric and conducting cylinders and spheres. The cylindrical vector wave functions are used to analyze scattering from cylinders [7, 8].

In wave propagation, the property of handedness, shown by chiral materials, is based upon the process of wave polarization, and is described in terms of helicity. E-polarization is counted which is perpendicular to the direction of propagation. If E-vector rotates clockwise, material is right handed, and vice versa [9]. The passage of linearly polarized electromagnetic wave through a chiral medium results two significant mechanisms, i.e. the magneto-coupling and optical rotation [9, 10]. According to the former property, electric and magnetic excitation give rise to both electric and magnetic polarization effect and the latter property has effect of cross polarization due to which linear polarized light rotates into circular polarized waves. Behind the medium, the two waves combine to yield a linearly polarized wave whose plane of polarization is rotated with respect to the plane of polarization of the incident light. This amount of rotation depends upon the distance travelled in the medium which implies that the optical activity is completely a medium phenomenon, and not just a surface impact [11, 12].

A random arrangement of helices into a medium whose permittivity and permeability is uniform gives rise to an isotropic chiral material. If all the helices in the material are arranged in the same direction, the material becomes an-isotropic i.e. directional dependent. This can be assembled by inserting small helices in the isotropic host medium in such a way that all the helices are oriented parallel to a fixed direction, but distributed randomly.

For the an-isotropic chiral medium, the electromagnetic fields satisfy the following constitutive relations [13]

$$\mathbf{D} = \bar{\bar{\boldsymbol{\epsilon}}} \cdot \mathbf{E} - \mathrm{j}\sqrt{\mu_0 \epsilon_0}\, \bar{\bar{\boldsymbol{\xi}}} \cdot \mathbf{H} \tag{1}$$

$$\mathbf{B} = \bar{\bar{\boldsymbol{\mu}}} \cdot \mathbf{H} + \mathrm{j}\sqrt{\mu_0 \epsilon_0}\, \bar{\bar{\boldsymbol{\xi}}} \cdot \mathbf{E} \tag{2}$$

with the medium parameter dyadics

$$\bar{\bar{\boldsymbol{\epsilon}}} = \epsilon_x \mathbf{a_x a_x} + \epsilon_t (\mathbf{a_y a_y} + \mathbf{a_z a_z})$$
$$\bar{\bar{\boldsymbol{\mu}}} = \mu_x \mathbf{a_x a_x} + \mu_t (\mathbf{a_y a_y} + \mathbf{a_z a_z})$$
$$\bar{\bar{\boldsymbol{\xi}}} = \xi \mathbf{a_x a_x}$$

Where ξ represents the chirality parameter. Here the axes $\mathbf{a}_x$ and $\mathbf{a}_y$ are transverse to z-axiswith $\mathbf{a}_x = \mathbf{a}_z \times \mathbf{a}_y$. They are selected so as to form the natural coordinates for the geometrical optics. The analytical formulation is given in section II, the differential scattering cross-sections are given in section III, the numerical results and the discussion are explained in section IV, and finally the conclusion is given in section V.

II. Analytical Formulation

Consider the geometry of a conducting circular perfect electric cylinder of radius 'a' coated with a uniaxial chiral layer so that the external radius is 'b' as shown in Fig. 1.

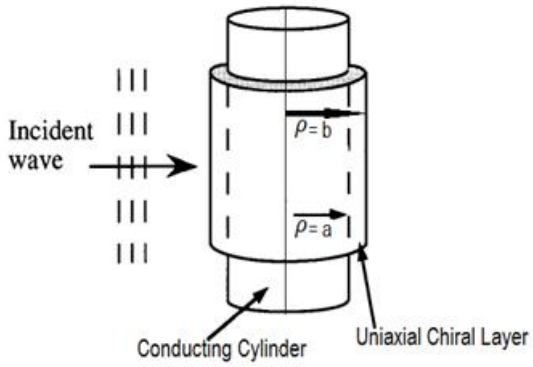

Fig. 1**:** A conducting cylinder coated with an anisotropic chiral material

Let η_c, k_+ and k_- are the chiral impedance and the wave numbers of the uniaxial chiral material respectively. For simplicity, we assumed the coordinate system so that the incident wave is travelling along the positive x-axis, and the axis of cylinder is coincident with z-axis as shown in Fig. 1.Since the arbitrary polarized waves TM^z and $TE^z$are independent and dual with each other, so TM^z incident case is considered without loss of generality [11]. The region outside the cylinder has been named as region 1 with $\rho > b$, and has wave number $k_0 = \omega\sqrt{\mu_0\varepsilon_0}$, while the region with uniaxial chiral layer has been named as region 2 with $a \le \rho \le b$, and has wave number $k_\pm = k_t\sqrt{A_\pm}$ with [14, 15]

$$k_t = \omega\sqrt{\mu_t\varepsilon_t}$$

$$A_\pm = \frac{1}{2}\left(\frac{\mu_z}{\mu_t} + \frac{\epsilon_z}{\epsilon_t}\right) \pm \sqrt{\frac{1}{4}\left(\frac{\mu_z}{\mu_t} - \frac{\epsilon_z}{\epsilon_t}\right)^2 + \frac{\xi^2\mu_0\varepsilon_0}{\mu_t\varepsilon_t}} \tag{3}$$

Where ε_z, ε_t and ε_0 are the axial permittivity, the transverse permittivity and the permittivity of free space respectively; while μ_z, μ_t and μ_0 are the axial permeability, the transverse permeability and the permeability of free space respectively. The expression (3) may be simplified using the following notations

$$E = \frac{\varepsilon_z}{\varepsilon_t} \quad , \quad M = \frac{\mu_z}{\mu_t} \quad , \quad K = \frac{\xi k_0}{k_t} \quad \text{and} \quad X = \sqrt{ME - K^2}$$

These quantities are assumed to have real values which presume the absence of losses in the uniaxial medium. Moreover, for X to be real, the inequality $\mu_z\varepsilon_z > \xi^2\mu_0\varepsilon_0$ is assumed to be valid which limits the magnitude of the chirality parameterξ. The values ofE, M, and X are assumed to be positive, and $A_\pm$ may be expressed as

$$A_\pm = \frac{1}{2}\left[M + E \pm \sqrt{(M-E)^2 + 4K^2}\right]$$
$$= \frac{1}{2}\left[M + E \pm \sqrt{(M+E)^2 - 4X^2}\right] \tag{4}$$

Let $\hat{\mathbf{e}}_\rho$, $\hat{\mathbf{e}}_\phi$ and $\hat{\mathbf{e}}_z$ be the unit base vectors of the circularly cylindrical co-ordinate system. Then, from the classical cylindrical Eigen modes $\mathbf{m}_n(k)$ and $\mathbf{n}_n(k)$ [7, 14], a set of uniaxial chiral wave functions can be constructed of the form, [7, 15]

$$\begin{Bmatrix} \mathbf{A}_n^{(q)}(k) \\ \mathbf{B}_n^{(q)}(k) \end{Bmatrix} = \frac{1}{\sqrt{2}}\left[\frac{in}{\rho}Z_n(k\rho)e^{in\phi}\hat{\mathbf{e}}_\rho - \frac{\partial Z_n(k\rho)}{\partial\rho}e^{in\phi}\hat{\mathbf{e}}_\phi \pm kZ_n(k\rho)e^{in\phi}\hat{\mathbf{e}}_z\right] \tag{5}$$

Where$q = 1, 2, 3, 4$ indicates that $Z_n(k\rho)$ becomes one of the Bessel functions $J_n(k\rho)$, $Y_n(k\rho)$, $H_n^{(1)}(k\rho)$ and $H_n^{(2)}(k\rho)$ respectively. Using these wave functions, the co-polar ($\mathbf{r}_n^{aa}$ and $\mathbf{r}_n^{bb}$) and cross-polar ($\mathbf{r}_n^{ab}$ and $\mathbf{r}_n^{ba}$) differential scattering coefficients for the uniaxial chiral coated layer can be derived.

The incident TM^z wave of unit amplitude of electric field can be expanded in terms of the circular cylindrical vector wave functions as [16]

$$\mathbf{E}_1^{\mathrm{i}} = \hat{\mathbf{e}}_z E_1 e^{-ik_0 x} = \hat{\mathbf{e}}_z E_1 e^{-ik_0(\rho\cos\phi)} = \sum_{n=-\infty}^{\infty} \mathbf{A}_n^{(1)}(k_0)$$

$$\mathbf{E}_1^{\mathrm{i}} = \sum_{n=-\infty}^{\infty}\left[\frac{jn}{\rho}J_n(k_0\rho)e^{jn\phi}\hat{\mathbf{e}}_\rho - \frac{\partial}{\partial\rho}J_n(k_0\rho)e^{jn\phi}\hat{\mathbf{e}}_\phi + k_0 J_n(k_0\rho)e^{jn\phi}\hat{\mathbf{e}}_z\right] \quad (6)$$

By Maxwell's equation, the corresponding component of incident magnetic field is [16]

$$\mathbf{H}_1^{\mathrm{i}} = \frac{1}{i\eta_0}\sum_{n=-\infty}^{\infty} \mathbf{A}_n^{(1)}(k_0)$$

$$\mathbf{H}_1^{\mathrm{i}} = \frac{1}{i\eta_0}\sum_{n=-\infty}^{\infty}\left[\frac{jn}{\rho}J_n(k_0\rho)e^{jn\phi}\hat{\mathbf{e}}_\rho - \frac{\partial}{\partial\rho}J_n(k_0\rho)e^{jn\phi}\hat{\mathbf{e}}_\phi + k_0 J_n(k_0\rho)e^{jn\phi}\hat{\mathbf{e}}_z\right] \quad (7)$$

Where $\eta_0 = \sqrt{\frac{\mu_0}{\epsilon_0}}$ represents the wave impedance of free space, and $J_n(k_0\rho)$ is the Bessel function of first kind. The scattered electric and magnetic fields in region 1, associated with the incident fields, may have both TM^z and TE^z components expressed as

$$\mathbf{E}_1^{\mathrm{r}} = \sum_{n=-\infty}^{\infty}\left[\mathbf{r}_n^{aa}\mathbf{A}_n^{(3)}(k_0) + \mathbf{r}_n^{ab}\mathbf{B}_n^{(3)}(k_0)\right]$$

$$\mathbf{E}_1^{\mathrm{r}} = \sum_{n=-\infty}^{\infty}\left\{\mathbf{r}_n^{aa}\left[\frac{jn}{\rho}H_n^{(1)}(k_0\rho)e^{jn\phi}\hat{\mathbf{e}}_\rho - \frac{\partial}{\partial\rho}H_n^{(1)}(k_0\rho)e^{jn\phi}\hat{\mathbf{e}}_\phi + k_0 H_n^{(1)}(k_0\rho)e^{jn\phi}\hat{\mathbf{e}}_z\right] + \mathbf{r}_n^{ab}\left[\frac{jn}{\rho}H_n^{(1)}(k_0\rho)e^{jn\phi}\hat{\mathbf{e}}_\rho - \frac{\partial}{\partial\rho}H_n^{(1)}(k_0\rho)e^{jn\phi}\hat{\mathbf{e}}_\phi - k_0 H_n^{(1)}(k_0\rho)e^{jn\phi}\hat{\mathbf{e}}_z\right]\right\} \quad (8)$$

$$\mathbf{H}_1^{\mathrm{r}} = \frac{1}{i\eta_0}\sum_{n=-\infty}^{\infty}\left[\mathbf{r}_n^{aa}\mathbf{A}_n^{(3)}(k_0) - \mathbf{r}_n^{ab}\mathbf{B}_n^{(3)}(k_0)\right]$$

$$\mathbf{H}_1^{\mathrm{r}} = \frac{1}{i\eta_0}\sum_{n=-\infty}^{\infty}\left\{\mathbf{r}_n^{aa}\left[\frac{jn}{\rho}H_n^{(1)}(k\rho_0)e^{jn\phi}\hat{\mathbf{e}}_\rho - \frac{\partial}{\partial\rho}H_n^{(1)}(k\rho_0)e^{jn\phi}\hat{\mathbf{e}}_\phi + k_0 H_n^{(1)}(k\rho_0)e^{jn\phi}\hat{\mathbf{e}}_z\right] - \mathbf{r}_n^{ab}\left[\frac{jn}{\rho}H_n^{(1)}(k\rho_0)e^{jn\phi}\hat{\mathbf{e}}_\rho - \frac{\partial}{\partial\rho}H_n^{(1)}(k\rho_0)e^{jn\phi}\hat{\mathbf{e}}_\phi - k_0 H_n^{(1)}(k\rho_0)e^{jn\phi}\hat{\mathbf{e}}_z\right]\right\} \quad (9)$$

Where $H_n^{(1)}(k\rho_0)$ is the Hankel function of first kind used to represent the out-going travelling wave, while $\boldsymbol{r}_n^{aa}$ and $\boldsymbol{r}_n^{ab}$ represent the scattering coefficients for the right circularly polarized (RCP) plane waves. According to the cylindrical vector wave functions in the uniaxial chiral material, the electric and magnetic fields within region 2 are

$$\boldsymbol{E}_2^c = \sum_{n=-\infty}^{\infty}\left[a_n\boldsymbol{A}_n^{(1)}(k_+) \pm b_n\boldsymbol{B}_n^{(1)}(k_-) + c_n\boldsymbol{A}_n^{(3)}(k_+) \pm d_n\boldsymbol{B}_n^{(3)}(k_-)\right]$$

$$\boldsymbol{E}_2^c = \sum_{n=-\infty}^{\infty}\left\{a_n\left[\frac{in}{\rho}J_n(k_+\rho)e^{in\phi}\hat{\boldsymbol{e}}_\rho - \frac{\partial}{\partial\rho}J_n(k_+\rho)e^{in\phi}\hat{\boldsymbol{e}}_\phi + k_+J_n(k_+\rho)e^{in\phi}\hat{\boldsymbol{e}}_z\right] + b_n\left[\frac{in}{\rho}J_n(k_-\rho)e^{in\phi}\hat{\boldsymbol{e}}_\rho - \frac{\partial}{\partial\rho}J_n(k_-\rho)e^{in\phi}\hat{\boldsymbol{e}}_\phi - k_-J_n(k_-\rho)e^{in\phi}\hat{\boldsymbol{e}}_z\right] + c_n\left[\frac{in}{\rho}H_n^{(1)}(k_+\rho)e^{in\phi}\hat{\boldsymbol{e}}_\rho - \frac{\partial}{\partial\rho}H_n^{(1)}(k_+\rho)e^{in\phi}\hat{\boldsymbol{e}}_\phi + k_+H_n^{(1)}(k_+\rho)e^{in\phi}\hat{\boldsymbol{e}}_z\right] + d_n\left[\frac{in}{\rho}H_n^{(1)}(k_-\rho)e^{in\phi}\hat{\boldsymbol{e}}_\rho - \frac{\partial}{\partial\rho}H_n^{(1)}(k_-\rho)e^{in\phi}\hat{\boldsymbol{e}}_\phi - k_-H_n^{(1)}(k_-\rho)e^{in\phi}\hat{\boldsymbol{e}}_z\right]\right\} \quad (10)$$

$$\boldsymbol{H}_2^c = \frac{1}{i\eta_0}\sum_{n=-\infty}^{\infty}\left[a_n\boldsymbol{A}_n^{(1)}(k_+) - b_n\boldsymbol{B}_n^{(1)}(k_-) + c_n\boldsymbol{A}_n^{(3)}(k_+) - d_n\boldsymbol{B}_n^{(3)}(k_-)\right]$$

$$\boldsymbol{H}_2^c = \frac{1}{i\eta_0}\sum_{n=-\infty}^{\infty}\left\{a_n\left[\frac{in}{\rho}J_n(k\rho_+)e^{in\phi}\hat{\boldsymbol{e}}_\rho - \frac{\partial}{\partial\rho}J_n(k\rho_+)e^{in\phi}\hat{\boldsymbol{e}}_\phi + k_+J_n(k\rho_+)e^{in\phi}\hat{\boldsymbol{e}}_z\right] - b_n\left[\frac{in}{\rho}J_n(k\rho_-)e^{in\phi}\hat{\boldsymbol{e}}_\rho - \frac{\partial}{\partial\rho}J_n(k\rho_-)e^{in\phi}\hat{\boldsymbol{e}}_\phi - k_-J_n(k\rho_-)e^{in\phi}\hat{\boldsymbol{e}}_z\right] + c_n\left[\frac{in}{\rho}H_n^{(1)}(k\rho_+)e^{in\phi}\hat{\boldsymbol{e}}_\rho - \frac{\partial}{\partial\rho}H_n^{(1)}(k\rho_+)e^{in\phi}\hat{\boldsymbol{e}}_\phi + k_+H_n^{(1)}(k\rho_+)e^{in\phi}\hat{\boldsymbol{e}}_z\right] - d_n\left[\frac{in}{\rho}H_n^{(1)}(k\rho_-)e^{in\phi}\hat{\boldsymbol{e}}_\rho - \frac{\partial}{\partial\rho}H_n^{(1)}(k\rho_-)e^{in\phi}\hat{\boldsymbol{e}}_\phi - k_-H_n^{(1)}(k\rho_-)e^{in\phi}\hat{\boldsymbol{e}}_z\right]\right\} \quad (11)$$

Where a_n, b_n, c_n and d_n represent the unknown scattering coefficients which can be found by using the appropriate boundary conditions at the inner and the outer uniaxial chiral layers, i.e. at $\rho = a$ and $\rho = b$. The boundary conditions at $\rho = a$ are

$$\left.\begin{matrix} E_2^c = 0 \\ H_2^c = 0 \end{matrix}\right\} \quad \rho = a, \quad 0 \le \phi \le 2\pi \quad (12)$$

The boundary conditions at $\rho = b$ are

$$\left.\begin{matrix} E_1^i + E_1^r = E_2^c \\ H_1^i + H_1^r = H_1^c \end{matrix}\right\} \quad \rho = b, \quad 0 \le \phi \le 2\pi \tag{13}$$

We obtained a system of six simultaneous equations as under

$$k_0 H_n^{(1)'}(k_0 b)\boldsymbol{r}_n^{aa} + k_0 H_n^{(1)'}(k_0 b)\boldsymbol{r}_n^{ab} - k_+ J_n'(k_+ b)a_n - k_- J_n'(k_- b)b_n - k_+ H_n^{(1)'}(k_+ b)c_n - k_- H_n^{(1)'}(k_- b)d_n = k_0 J_n'(k_0 b) \tag{14}$$

$$k_0 H_n^{(1)}(k_0 b)\boldsymbol{r}_n^{aa} - k_0 H_n^{(1)}(k_0 b)\boldsymbol{r}_n^{ab} - k_+ J_n(k_+ b)a_n + k_- J_n(k_- b)b_n - k_+ H_n^{(1)}(k_+ b)c_n + k_- H_n^{(1)}(k_- b)d_n = k_0 J_n(k_0 b) \tag{15}$$

$$k_0 H_n^{(1)'}(k_0 b)\boldsymbol{r}_n^{aa} - k_0 H_n^{(1)'}(k_0 b)\boldsymbol{r}_n^{ab} - \frac{\eta_0}{\eta_c} k_+ J_n'(k_+ b)a_n + \frac{\eta_0}{\eta_c} k_- J_n'(k_- b)b_n - \frac{\eta_0}{\eta_c} k_+ H_n^{(1)'}(k_+ b)c_n + \frac{\eta_0}{\eta_c} k_- H_n^{(1)'}(k_- b)d_n = -k_0 J_n'(k_0 b) \tag{16}$$

$$k_0 H_n^{(1)}(k_0 b)\boldsymbol{r}_n^{aa} + k_0 H_n^{(1)}(k_0 b)\boldsymbol{r}_n^{ab} - \frac{\eta_0}{\eta_c} k_+ J_n(k_+ b)a_n - \frac{\eta_0}{\eta_c} k_- J_n(k_- b)b_n - \frac{\eta_0}{\eta_c} k_+ H_n^{(1)}(k_+ b)c_n - \frac{\eta_0}{\eta_c} k_- H_n^{(1)}(k_- b)d_n = -k_0 J_n(k_0 b) \tag{17}$$

$$k_+ J_n'(k_+ a)a_n + k_- J_n'(k_- a)b_n + k_+ H_n^{(1)'}(k_+ a)c_n + k_- H_n^{(1)'}(k_- a)d_n = 0 \tag{18}$$

$$k_+ J_n(k_+ a)a_n - k_- J_n(k_- a)b_n + k_+ H_n^{(1)}(k_+ a)c_n - k_- H_n^{(1)}(k_- a)d_n = 0 \tag{19}$$

The set of these equations yields a matrix of order 6×6 in terms of unknown scattering coefficients. The solution of this matrix, which can be solved by Cramer's rule, gives the unknown scattering coefficients.

III. Scattering Cross-Section

The differential scattering cross-sections per unit length for the right circular co-polarized and cross-polarized (RCP) plane waves can be written as [16]

$$\left.\frac{d\sigma}{d\phi}\right|_{RCP\to RCP} = \frac{2}{\pi k_0}\left|\sum_{n=-\infty}^{\infty} \boldsymbol{r}_n^{aa} e^{in\phi}\right|^2 \tag{20}$$

$$\left.\frac{d\sigma}{d\phi}\right|_{RCP\to LCP} = \frac{2}{\pi k_0}\left|\sum_{n=-\infty}^{\infty} \boldsymbol{r}_n^{ab} e^{in\phi}\right|^2 \tag{21}$$

The differential scattering cross-sections per unit length for the left circular co-polarized and cross-polarized (LCP) plane waves can be written as

$$\left.\frac{d\sigma}{d\phi}\right|_{LCP\to RCP} = \frac{2}{\pi k_0}\left|\sum_{n=-\infty}^{\infty} \mathbf{r}_n^{ba} e^{in\phi}\right|^2 \tag{22}$$

$$\left.\frac{d\sigma}{d\phi}\right|_{LCP\to LCP} = \frac{2}{\pi k_0}\left|\sum_{n=-\infty}^{\infty} \mathbf{r}_n^{bb} e^{in\phi}\right|^2 \tag{23}$$

IV. Numerical Results And Discussion

The numerical results are based upon the analytical formulations for PEC circular cylinder coated with uniaxial chiral layer of constant as well as varying thickness. The differential scattering cross-sections for right circular co-polarized and cross-polarized plane waves, given by equations (20) and (21), for uniaxial chiral coated conducting cylinder have been plotted as functions of scattering angle in all the plots. The differential scattering cross sections for left circular co-polarized and cross-polarized plane waves may be determined is a similar way. The radius of the conducting cylinder has been chosen for simulation to be $k_0 a = 0.60\,\pi$, while the radius of the uniaxial chiral coating layer is $k_0 b = 0.90\,\pi$. For the lossless case, the permittivity has been chosen as $\varepsilon = 4\varepsilon_0$, while the permeability is $\mu = \mu_0$. For the lossy permittivity case, the permittivity is $\varepsilon = (4 + 2i)\varepsilon_0$, while the permeability is $\mu = \mu_0$. For the lossy permeability case, the permittivity is $\varepsilon = 2\varepsilon_0$, while that of permeability is $\mu = (2 + i)\mu_0$.

Fig. 2, (a. & b.) shows the variation of differential scattering cross section of the co- and cross-polarized components with change in values of scattering angle for a uniaxial chiral coated cylinder for lossless case with unit value of chirality. As the thickness of the chiral coating increases, the value of differential scattering cross section for the co-polar components goes on decreasing as a function of the scattering angle; while for the cross components, the value of differential scattering cross section has different values for small values of scattering angle, but has almost the same increasing values for the larger values of scattering angle.

Fig.3and fig.4show the comparison between co-polar and cross-polar components of the scattered field respectively by a PEC uniaxial chiral coated cylinder for $\xi = 0$, $\varepsilon_t = \varepsilon_z = \varepsilon_0$ and $\mu_t = \mu_z = \mu_0$ which tends to PEC chiral coated cylinder of the published literature [11]. Fig. 5 and fig. 6 show the variations of differential scattering cross-section with respect to the scattering angle for the right circularly co-polarized and cross polarized plane wave for different values of chirality i.e. $\xi = 0.0,\ 0.5$ and 1.0 for the lossless, lossy permittivity and lossy permeability cases respectively. It is observed in fig. 5 that the differential scattering cross section per unit scattering angle splits with increase of uniaxial chirality, because due to presence of scatterers of different size, the resonance occurs. It is also noted that for any of the two values of scattering angle, the

differential scattering cross section has the least value. Since the incident wave is travelling along positive x-axis, so the scattering pattern has a maximum in the forward direction i.e. $\phi = 0^{\circ}$. It is shown in fig. 6 that the scattering maximum pattern in the forward direction goes on decreasing with increase of chirality. For scattering angle up to 90°, the differential scattering cross-section per unit scattering angle splits a little bit, but for larger scattering angle, no splitting occurs and the differential scattering cross section has almost constant higher values for different values of chirality.

Fig. **7** and fig. 8 show the comparison of co-components with the cross-components for the variation of differential scattering cross section with the change in the value of the scattering angle for different values chirality for the lossless and lossy permittivity cases. For different values of chirality, we have approximately same co and cross components. It is noted that as the scattering angle increases, the differential scattering cross section falls rapidly to a minimum value; but for large values of scattering angle and with increase of chirality, the resonance effect keeps on increasing and the splitting occurs. The peaks of the cross components shift to higher values as the value of ϕ increases with no splitting and resonance effects.

Fig. 9 shows the comparison of the results of scattering behavior of uniaxial chiral material with a chiral one for the variation of differential scattering cross section with the change in value of scattering angle for different values of chirality for the lossless case. Due to the isotropic property of chiral material, the differential scattering cross section per unit scattering angle splits and the resonance occurs; whereas due to the anisotropic property of uniaxial chiral material, only a little bit splitting in observed. Moreover the uniaxial chiral PEC cylinder has only one value of scattering angle where the differential scattering cross section has the minimum value.

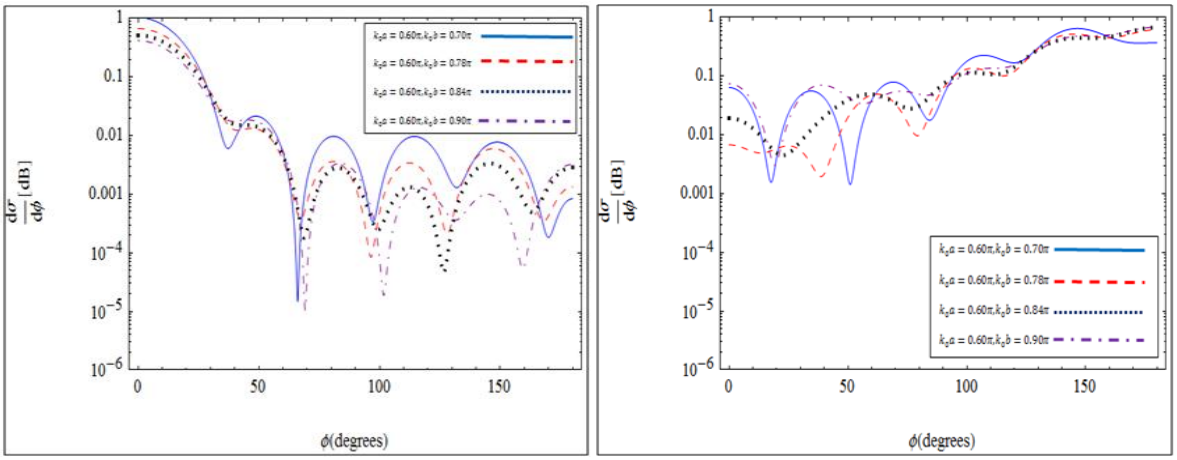

a. Co-polar b. Cross-polar

Fig. 2 (a, b): Variation of differential scattering cross section of the co- and cross-polarized components with change in values of scattering angle for a uniaxial chiral coated cylinder of varying thickness (chirality=1, Lossless case).

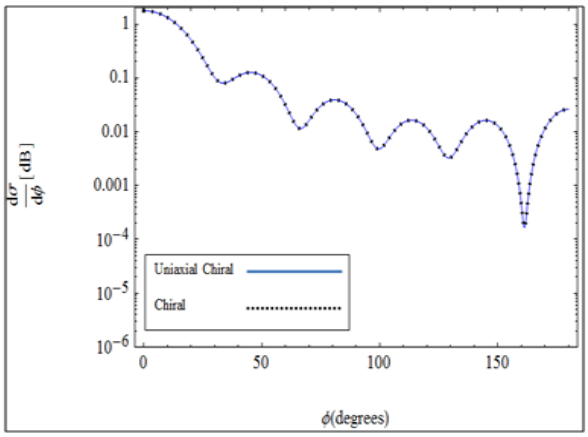

Fig. 3: Comparison of co-polar components of the scattered field with Liu & Jaggard work (where $\xi = 0.0, \mu = \mu_0, \varepsilon = 4\varepsilon_0$)

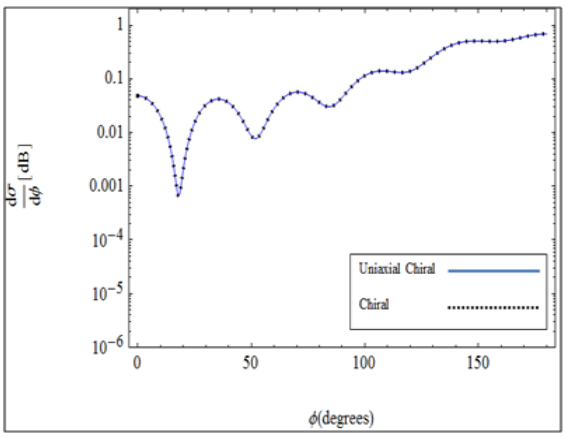

Fig. 4: Comparison of cross-polar components of the scattered field with Liu & Jaggard work (where $\xi = 0.0, \mu = \mu_0, \varepsilon = 4\varepsilon_0$)

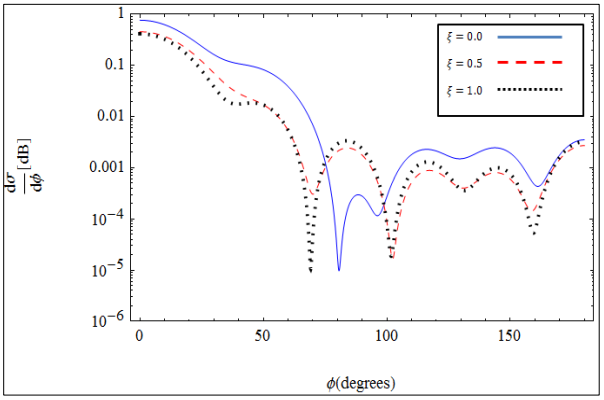

a. Lossless Case

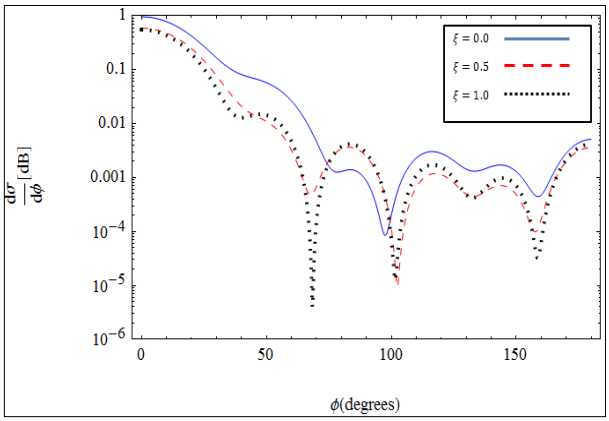

b. Lossy Permittivity Case

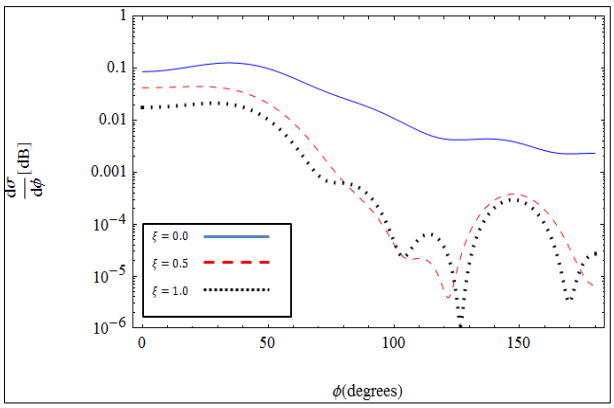

c. Lossy Permeability Case

Fig. 5 (a, b, c): Variation of differential scattering cross section of the Co-components with the change in the value of scattering angle ϕ (degrees)

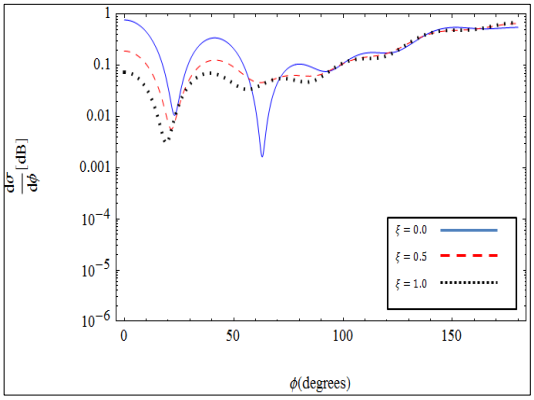

a. Lossless Case

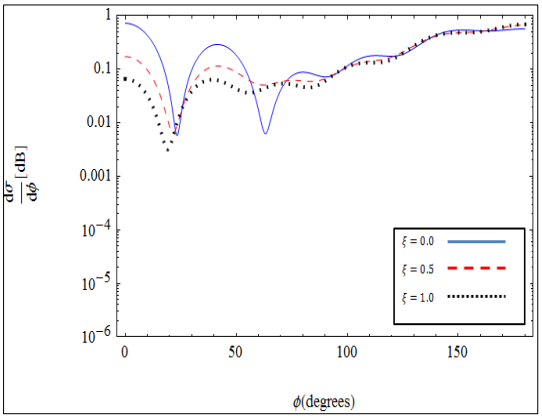

b. Lossy Permittivity Case

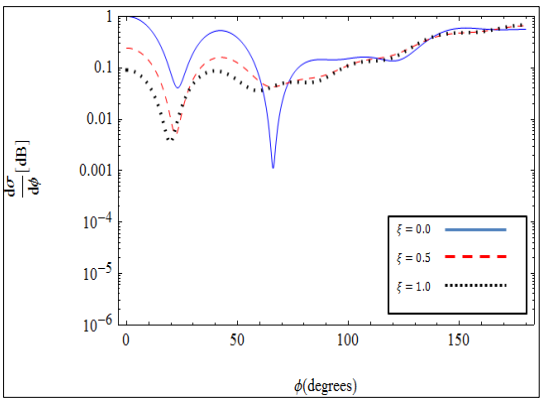

c. Lossy Permeability Case

Fig.6 (a, b, c): Variation of differential scattering cross section of the Cross-components with the change in the value of scattering angle ϕ (degrees)

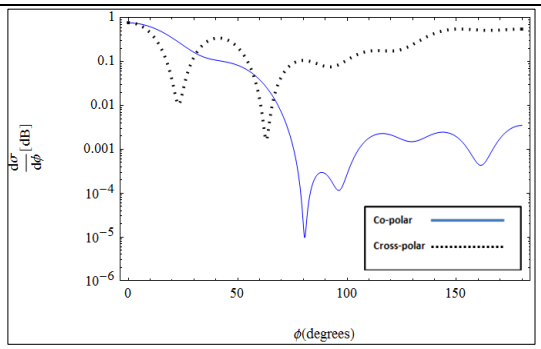

a. $\xi = 0.0$

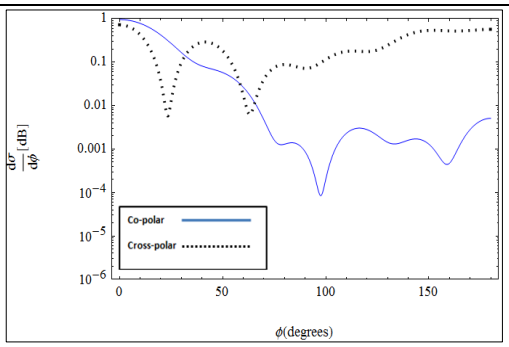

a. $\xi = 0.0$

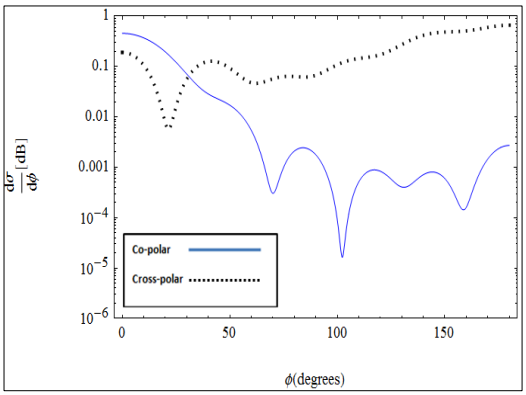

b. $\xi = 0.5$

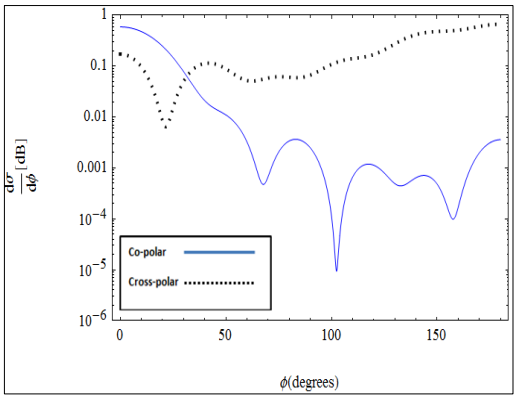

b. $\xi = 0.5$

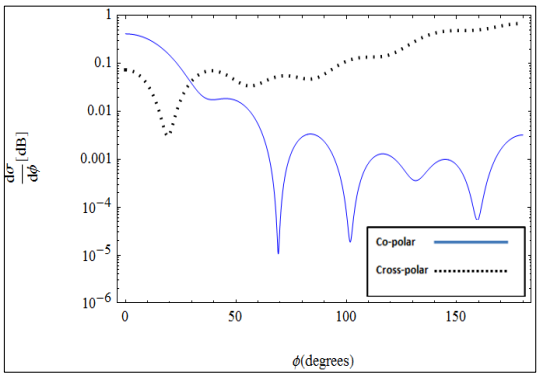

c. $\xi = 1.0$

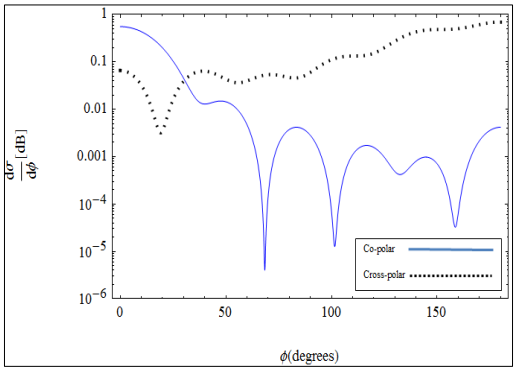

c. $\xi = 1.0$

Fig. 7 (a, b, c): Comparison of co-components with cross-components for the variation of differential scattering cross section with the change in value of scattering angle for different values of chirality. (Lossless Case)

Fig. 8 (a, b, c): Comparison of co-components with cross-components for the variation of differential scattering cross section with the change in value of scattering angle for different values of chirality. (Lossy Permittivity Case)

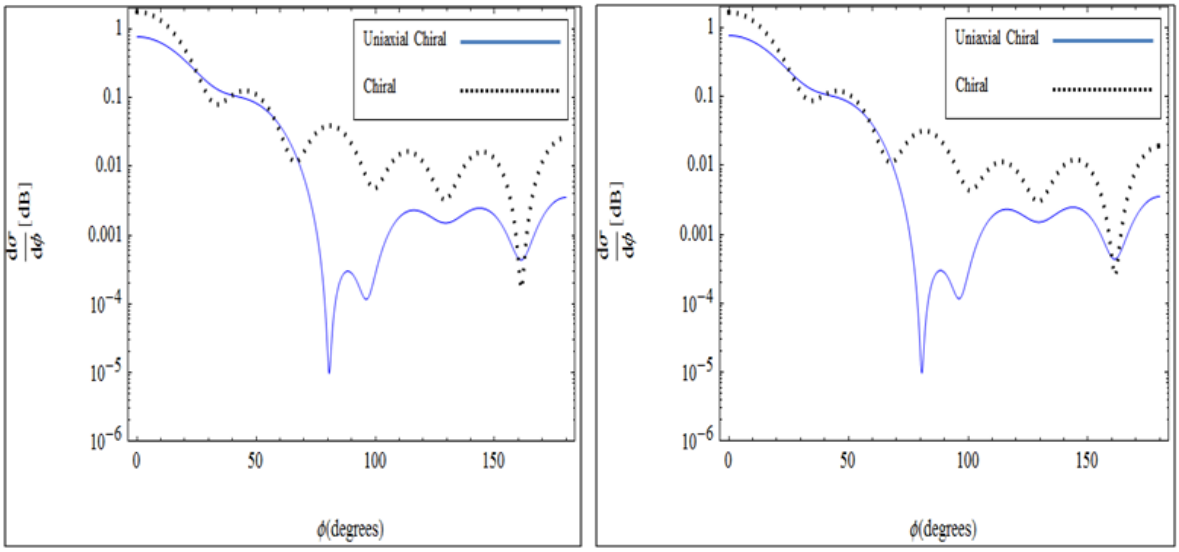

a. $\xi = 0.0$ b. $\xi = 0.5$

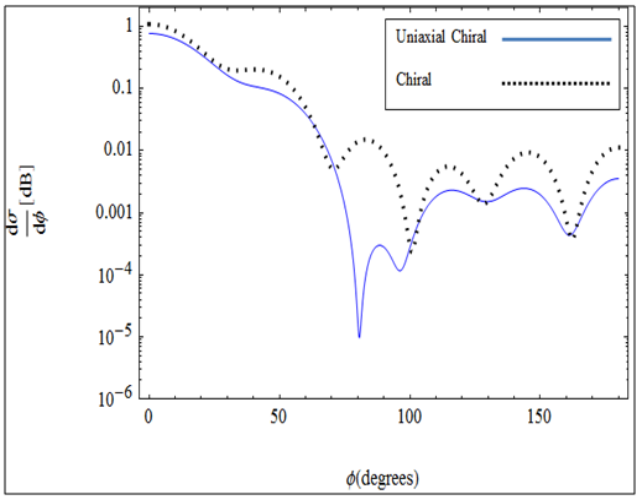

c. $\xi = 1.0$

Fig. 9 (a, b, c): Comparison of the results of uniaxial chiral with chiral material for the variation of differential scattering cross section with the change in value of scattering angle for different values of chirality. (Lossless Case)

V. Conclusion

In present paper, the Eigen wave functions are developed to scrutinize the electromagnetic scattering from uniaxial chiral coated conducting cylinder using Mie's approach. It is observed that uniaxial chirality in an object affects significantly the scattering properties of the scatterers and the nulls of the scattering pattern shift according to their polarization due to the presence of different wave numbers. The addition of uniaxial chirality produces the circular birefringence which is evident from the splitting of co- and cross-polar scattering cross sections. It is also perceived that splitting and resonance effects in scattered wave from uniaxial chiral layer are much less than that from a chiral layer. That's the reason the uniaxial chiral medium is recommended for the design of reflection-reduction curved surfaces in a wide band frequency range.

References

[1] S. Bassiri, C. H. Papas and Nader Engheta, "Electromagnetic Wave Propagation through a Dielectric Chiral Interface and Through a Chiral Slab", Journal of Optical Society of America, Vol. 5, pp. 9, September 1988.
[2] J. Viitanen and I. V. Lindell, "Uniaxial chiral quarter-wave polarization transformer", Electron. Letter, Vol. 29, pp. 1074-1075, June 1993.
[3] V. Lindell and A. H. Sihvola, "Plane-wave reflection from uniaxial chiral interface and its application to polarization transformation", IEEE Trans. Antennas Propagation, Vol. 43, pp. 1397-1404, Dec. 1995.
[4] Priou (ed.), Bianisotropic and Biisotropic Media and Applications (EMW Publisher, Boston, 1994).
[5] Vande Hulst H C, Light Scattering by Small Particles (McGraw Hill, New York, 1941).
[6] Mie G, "Beitr¨ agezur Optiktr¨ uber Medien, spezell kolloidalev Metall¨osunger Ann.", Phys. 25, pp. 377–445, 1908.
[7] Stratton, J. A. Electromagnetic Theory (New York, McGraw Hill, 1941).

[8] Dajun Cheng, G. Wang and Y. Jin, "Electromagnetic Scattering Response from a Uniaxial Chiral Cylinder by using Cylindrical Vector Wave Functions", Science in China, Vol. 41, No. 3, June 1998.
[9] Bassiri S, "Electromagnetic Wave Propagation and Radiation in Chiral Media", doctoral diss., California Institute of Technology, Pasadena, California, 1987.
[10] Dong, J. F. and J. Li, "The reflection and transmission of electromagnetic waves by a uniaxial chiral slab", Progress In Electromagnetics Research, Vol. 127, pp. 389-404, 2012.
[11] Huang, C., J. Zhao, T. Jiang, and Y. Feng, "Asymmetric transmission of linearly polarized electromagnetic wave through chiral metamaterial structure", Journal of Electromagnetic Waves and Applications, Vol. 26, pp. 1192–1202, 2012.
[12] D. L. Jaggard, A. R. Michelson, and C. H. Papas, "On electromagnetic waves in chiral media", Applied Physics, Vol. 18, pp. 211-216, 1978.
[13] Lindell, I. V. and A.H. Sihvola, "Plane-wave reflection from uniaxial chiral interface and its application to polarization transformation", IEEE Transactions on Antennas and Propagation, Vol. 43, No. 12, 1995.
[14] Cheng, D., Y. M. M. Antarand and G. Wang, "Electromagnetic scattering by a cylinder coated with a uniaxial chiral layer of varying thickness", Journal of Physics Communications, 125(2000), pp. 90-104, 2000.
[15] Ghaffar, A., M. H. Shahzad, M. Y. Naz, S. Ahmed, Q. A. Naqvi, A. A. Syed, and M. Sharif, "Analysis of electromagnetic field trans-mitted by a uniaxial chiral lens", Journal of Electromagnetic Waves and Applications, Vol. 26, pp. 1007-1017, 2012.
[16] C. Liu and D. L. Jaggard, "Mueller Matrices for Scattering from Chiral coated Curved Surfaces", Progress in Electromagnetic Research, PIER 12, pp. 303-333, 1996.